

OPTICAL PROPERTIES OF TIN AT HELIUM TEMPERATURES

A. I. GOLOVASHKIN and G. P. MOTULEVICH

P. N. Lebedev Physics Institute, Academy of Sciences, U.S.S.R.

Submitted to JETP editor February 11, 1964

J. Exptl. Theoret. Phys. (U.S.S.R.) 47, 64-72 (July, 1964)

The optical constants of tin were measured at temperatures of 4.2, 78 and 293°K in the wavelength range 0.9–12μ. The temperature dependence of the electron-phonon collision frequency was determined in the case of high-energy light quanta. The experimental results confirmed the theoretical results derived from the quantum transport equation.

THE optical constants of metals depend strongly on the conduction electron density as well as on the interaction of electrons with phonons. At low temperatures, the electron-phonon collision frequency  $\nu^{ef}$  in the case of high-energy light quanta  $\hbar\omega$  differs strongly from the classical collision frequency  $\nu_{cl}^{ef}$  which occurs in the static conductivity. This problem was discussed in the work of Gurzhi,<sup>[1]</sup> who derived a quantum transport equation and obtained the temperature dependence  $\nu^{ef}(T)$  in the infrared region of the spectrum. The quantum transport equation makes the frequency  $\nu^{ef}$  a finite quantity, equal to  $\frac{2}{5}\nu(\Theta)$ , at absolute zero ( $T = 0$ ), so that it does not tend to zero—as would follow from the classical transport equation. The parameter  $\nu(\Theta)$  is found from the relationship valid at  $T \gg \Theta$ :

$$\nu^{ef}(T) = \nu_{cl}^{ef}(T) = \nu(\Theta) T/\Theta.$$

The finite value of  $\nu^{ef}$  at  $T = 0$  is due to the fact that, although at this temperature an electron cannot absorb phonons which are absent, it can—having a high energy equal to  $\hbar\omega$ , if  $\hbar\omega > k\Theta$ —create the complete spectrum of phonons. Here,  $\omega$  is the angular frequency of the light vibrations,  $\Theta$  is the Debye temperature,  $\hbar$  is Planck's constant,  $k$  is Boltzmann's constant.

Figure 1, taken from Gurzhi's dissertation,<sup>[1]</sup> gives the dependence  $\nu^{ef}(T)$ . The upper curve was obtained using the quantum transport equation, and the lower using the classical transport equation. At  $T \gg \Theta$ , the results of the classical and quantum equations are identical. At  $T \approx \Theta$ , the difference between them is slight, and only at  $T \ll \Theta$  is there a considerable divergence between the results.

The finite value of  $\nu^{ef}(0)$  gives rise to a finite absorption of light at  $T = 0$ . By measuring the temperature dependence of the optical constants,

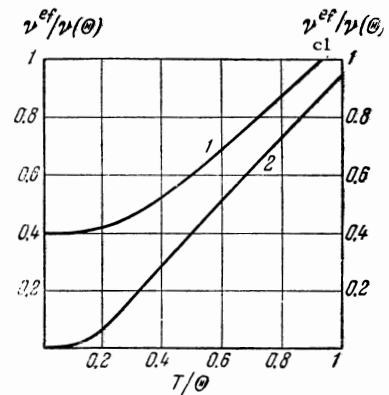


FIG. 1. Temperature dependence of the electron-phonon collision frequency: 1) for  $\nu^{ef}/\nu(\Theta)$ ; 2) for  $\nu_{cl}^{ef}/\nu(\Theta)$ .

we can determine the temperature dependence  $\nu^{ef}(T)$ . It follows that to check the theory we need to carry out measurements at sufficiently low temperatures.

It should be mentioned that the finite absorption at  $T = 0$  may also be due to an effect associated with the surface losses (the anomalous skin effect). Obviously, to check the temperature dependence of  $\nu^{ef}$  we must study metals in which the magnitude of surface losses is small compared with the volume ones.

Our earlier measurements of the optical constants of tin at temperatures of 293 and 78°K<sup>[2]</sup> have shown that tin is a very suitable subject for such a study. Therefore, in the present work we measured the optical constants of tin at  $T = 4.2^\circ\text{K}$  in the wavelength range 0.9–12μ and repeated the measurements of the optical properties of tin at 293 and 78°K. The results obtained at room and nitrogen temperatures were identical with the earlier results. To check the theory, we need to measure two quantities (in our case  $n$  and  $\kappa$ ) over a sufficiently wide range of wavelengths. Only such measurements allow us to separate the surface

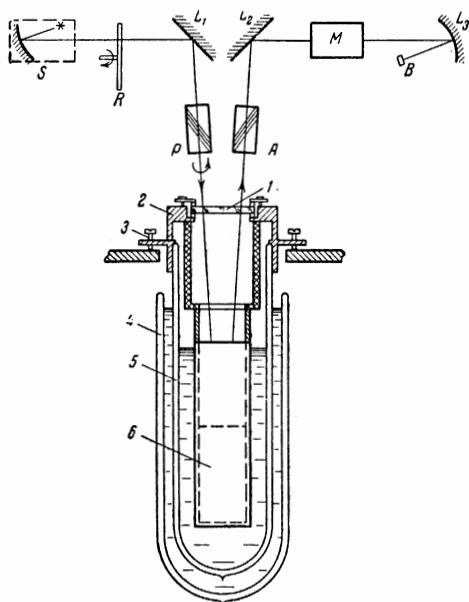


FIG. 2a. Experimental layout: S is the light source, R is the chopper,  $L_1$  and  $L_2$  are the plane mirrors, P is the polarizer, A is the analyzer, M is the monochromator,  $L_3$  is the spherical mirror, and B is the bolometer; 1) the rocksalt window sealed with rubber gaskets; 2) the cap; 3) the support screws; 4) the nitrogen Dewar; 5) the helium Dewar; 6) the mount with the test mirrors in a jacket. The chopper R was removed when the rotating polarizer P was employed. When the chopper was used the polarizer was not rotated.

losses from the volume ones and to compare the theory with experiment.

1. Measurement of the optical constants was carried out using apparatus which was in principle identical with that used by us in the earlier work.<sup>[2,3]</sup> To determine the optical constants  $n$  and  $\kappa$  ( $n - i\kappa$  is the complex refractive index) at a given wavelength  $\lambda$ , it is sufficient to determine the angle of incidence  $\varphi$  of light on a mirror, the phase shift  $\Delta$  between the p- and s-components of the reflected light and the azimuth  $\rho$ . In our apparatus, the angle of incidence  $\varphi$  was fixed. We used eight reflections of light from the test mirrors. We determined  $\lambda$  and  $\rho$  corresponding to the null signal in the set-up shown in Fig. 2a. Then  $\Delta_8 = k\pi/2$ , where  $\Delta_8$  is the total phase shift after eight reflections,  $k = 1, 2, \dots$ . For odd  $k$ , we used a rotating selenium polarizer P, and the azimuth  $\rho_8$  was determined with an analyzer A ( $\rho_8$  is the azimuth obtained after eight reflections from the test mirrors). For even  $k$ , we used an additional chopper R, placed the analyzer A at an angle of  $45^\circ$  and measured the azimuth  $\rho_8$  with the polarizer P.

There were two test mirrors (L in Fig. 2b), which were placed exactly parallel to each other. After four reflections from the test mirrors, the

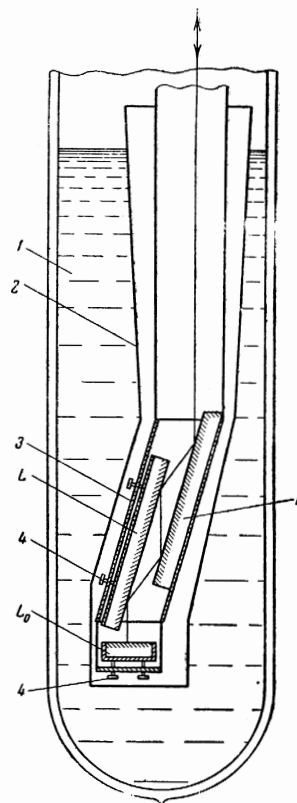


FIG. 2b. Low-temperature part of the apparatus: L are the test mirrors,  $L_0$  is the mirror that reflects back the beam; 1) helium; 2) the jacket; 3) the mount; 4) the adjusting screws of the mount. This figure gives the section at right angles to that in Fig. 2a.

light beam was reflected back by a mirror  $L_0$ , suffered four more reflections from the test mirrors, passed through the analyzer and a monochromator and fell on a bolometer. The mirror  $L_0$  separated the beams incident on and reflected from it by  $4^\circ$  in a plane perpendicular to the plane of incidence. The angles of incidence on the test mirrors were  $75-81^\circ$ .

Our apparatus included, apart from the test mirrors L, mirrors  $L_1$  and  $L_0$  which could in principle make some contribution to the phase shift and the azimuth of the investigated signal. The influence of the mirror  $L_0$ , which turned the beam by  $4^\circ$ , was negligibly small, but the influence of the mirror  $L_1$  was somewhat greater. This influence was taken into account although the correction for it was less than 1% over the whole range of wavelengths.

The test mirrors were placed in a mount having locating springs (Fig. 2b). The mirrors were rendered parallel with an accuracy better than  $1'$  by means of adjusting screws. The mount was suspended in a cap by means of plates of stainless steel and Plexiglas. Transverse spacers made the whole structure sufficiently rigid. With this

Table I. Optical constants of tin

$\lambda, \mu$	$T = 293^\circ \text{K}$		$T = 78^\circ \text{K}$		$T = 4,2^\circ \text{K}$	
	$n$	$\kappa$	$n$	$\kappa$	$n$	$\kappa$
0.93	3.15	7.28	3.43	7.17	2.95	7.62
0.99	3.44	7.34	3.92	6.94	3.70	7.15
1.2	3.76	7.63	3.53	6.45	3.05	5.98
1.35	3.57	8.04	2.76	6.99	2.55	6.64
1.5	3.31	8.67	2.09	7.98	1.99	7.80
1.7	3.13	9.88	1.75	9.29	1.51	9.35
2.0	3.10	11.8	1.65	11.4	1.38	11.4
2.5	3.63	14.8	1.69	14.6	1.39	14.6
3.0	4.41	17.8	1.88	18.0	1.58	18.0
3.5	5.27	20.5	2.13	21.1	1.95	21.1
4.0	6.19	23.2	2.46	24.2	2.13	24.2
5.0	8.49	28.5	3.75	29.7	2.75	30.0
6.0	11.0	33.1	4.97	35.5	3.73	35.8
7.0	13.8	37.1	6.51	41.4	4.89	41.6
8.0	16.6	40.6	8.17	47.0	6.05	47.4
9.0	19.3	43.8	10.0	51.7	7.90	53.3
10.0	22.0	46.4	12.4	55.8	10.1	58.7
11.0	24.8	49.0	15.7	59.8	12.6	63.4
12.0	27.8	51.6	18.2	63.8	15.3	67.0

type of suspension, the heat leak along these plates was negligible when helium was used. The total heat leak was such that a Dewar of 3–4 liters was sufficient for 4–5 hours work. The mount together with the mirrors was placed in a jacket in order to prevent the test mirrors from coming into direct contact with liquid helium. The helium level in the Dewar during measurements was considerably higher than the mirror positions. Thus the mirrors were in a helium vapor environment and their temperature was practically identical with that of liquid helium. The light was incident on the mirrors from above and it passed through the cap. Polished rock-salt plates, 5–6 mm thick were used as windows. The windows were sealed by means of rubber gaskets. By taking special precautions (blowing nitrogen, covering during filling up, drying with silica gel, etc.), one rock-salt window could be used 4–5 times or more. The construction of the helium part of the optical system avoided the need for complex optical Dewars and made it possible to work with the usual glass Dewars of 80–120 mm diameter.

The system including the cap, the mount with the test mirrors, and the Dewars, was attached by two support screws to a baseplate. The position of this system with respect to other parts of the apparatus was firmly fixed. This was checked by special tests. Moreover, a check of the constancy of the adjustment of the whole system was provided by the identity of the results of the measurements of the optical constants at room temperature, which were carried out before filling with helium and after heating. The sequence of measurements of the optical constants was as follows: using the same mirrors, we measured the optical constants

first at room temperature, then at the temperature of liquid helium, then again at room temperature, and, finally, at the temperature of liquid nitrogen. The adjustment carried out at the beginning of the tests was retained very well during subsequent measurements. During the measurements at room temperature and at helium temperature the test mirrors were in a helium atmosphere.

The mirrors were prepared by evaporating tin in vacuum  $[(5-6) \times 10^{-6} \text{ mm Hg}]$  on to a glass substrate. The evaporation conditions were similar to those used in [2]. The electrical properties and the density were the same as those of the layers used in the earlier work. [2]

2. The results of our measurements are listed in Table I and shown in Figs. 3 and 4. They are the average values for seven sets of mirrors. For each set with the same mirror positions, we measured the optical constants at helium, nitrogen, and room temperatures. The results referring to the nitrogen and room temperatures were identical with those obtained earlier. [2]

In determining the optical constants listed in Table I, we took into account the dependence of the surface impedance on the angle of incidence. This dependence was very weak and, therefore, we used only the terms which were linear with respect to  $\sin^2 \varphi / (n^2 + \kappa^2)$ . The constants  $n$  and  $\kappa$  were determined using the following formulas:

$$n = n_0 \left( 1 + \frac{\sin^2 \varphi}{2(n_0^2 + \kappa_0^2)} \right), \quad n_0 = \frac{\sin \varphi \tan \varphi \cos 2\rho}{(1 - \sin 2\rho \cos \Delta)}; \quad (1)$$

$$\kappa = \kappa_0 \left( 1 - \frac{\sin^2 \varphi}{2(n_0^2 + \kappa_0^2)} \right), \quad \kappa_0 = \frac{\sin \varphi \tan \varphi \sin 2\rho \sin \Delta}{(1 - \sin 2\rho \cos \Delta)}. \quad (2)$$

The correction for the dependence of the surface

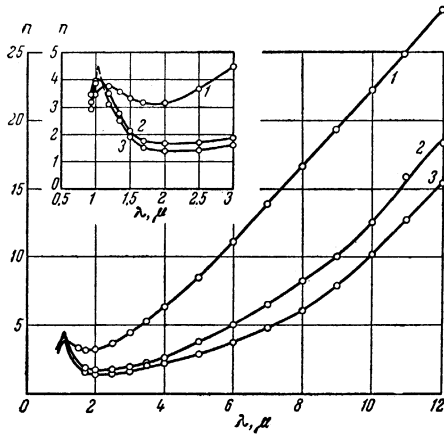


FIG. 3. Dependence of  $n$  on  $\lambda$ : 1)  $T = 293^\circ\text{K}$ ; 2)  $T = 78^\circ\text{K}$ ; 3)  $T = 4.2^\circ\text{K}$ .

impedance on  $\varphi$  amounted to about 1% in the region of  $\lambda = 1 \mu$ , 0.3% in the region of  $\lambda = 2 \mu$  and was negligibly small in the region  $\lambda > 2 \mu$ .

From the data in Table I, it follows that tin exhibits a weak anomalous skin effect over the whole investigated range of temperatures. Even at  $T = 4.2^\circ\text{K}$ , the surface losses amount to 15–20% of the total loss. Therefore, the results were analyzed using the method employed earlier in [2]. In this analysis, we used the wavelength range 3–12  $\mu$  in which the internal photoeffect contribution to the optical constants could be neglected.<sup>1)</sup>

In the analysis of the results, we used the formulas

$$N = \frac{0.1115 \cdot 10^{22} (n^2 + \kappa^2)^2}{\lambda^2 (\kappa^2 - n^2)} (1 - \beta_1)^{-1}, \quad (3)$$

$$\frac{\nu_{\text{opt}}}{N} = 1.690 \cdot 10^{-6} \lambda \frac{2n\kappa}{(n^2 + \kappa^2)^2} (1 - \beta_2), \quad (4)$$

$$\beta_1 = \frac{3v}{8c} \kappa \left[ \frac{1 + (n/\kappa)^2}{1 + (\nu_{\text{opt}}/\omega)^2} \right]^{1/2} \times \left[ \cos(\varphi_1 - \varphi_2) + \frac{2n\kappa}{\kappa^2 - n^2} \sin(\varphi_1 - \varphi_2) \right], \quad (5)$$

<sup>1)</sup>The experimental results for the 0.9–3  $\mu$  region allow us to estimate the interband transition energy for tin. An estimate of this quantity, obtained using the maximum slope of the dependence of  $\kappa/\lambda$  on  $\omega$ , gives the following values:  $\Delta E = 1.2 \text{ eV}$  for  $T = 295^\circ\text{K}$  and  $\Delta E = 1.3 \text{ eV}$  for  $T = 4.2^\circ\text{K}$ . The dependence of  $\kappa/\lambda$  on the energy of the light quanta is very steep in this region of energies. This applies particularly to the results at helium temperature. Therefore, in determining the values of  $\Delta E$ , we may, in the first approximation, neglect the small contribution of free electrons. These values of the interband transition energy are close to the energy of the corresponding transition in gray tin ( $\Delta E = 1.28 \text{ eV}$ ). [4].

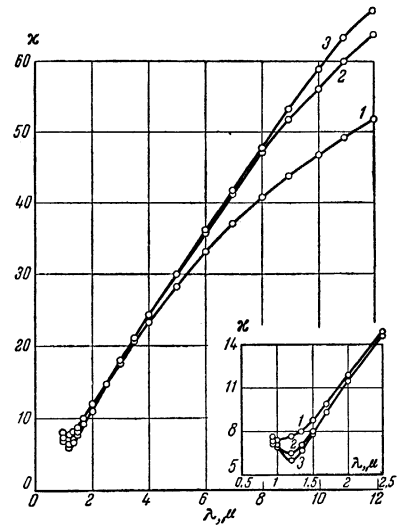


FIG. 4. Dependence of  $\kappa$  on  $\lambda$ : 1)  $T = 293^\circ\text{K}$ ; 2)  $T = 78^\circ\text{K}$ ; 3)  $T = 4.2^\circ\text{K}$ .

$$\beta_2 = \frac{3v}{8c} \kappa \left[ \frac{1 + (n/\kappa)^2}{1 + (\nu_{\text{opt}}/\omega)^2} \right]^{1/2} \times \left[ \cos(\varphi_1 - \varphi_2) - \frac{\kappa^2 - n^2}{2n\kappa} \sin(\varphi_1 - \varphi_2) \right]. \quad (6)$$

Here,  $\tan \varphi_1 = n/\kappa$ ,  $\tan \varphi_2 = \omega/\nu_{\text{opt}}$ ,  $\lambda$  is the wavelength of light in microns,  $c$  is the velocity of light in vacuum,  $N$  is the conduction electron density,  $\nu_{\text{opt}}$  is the frequency of electron collisions found from the optical data,  $v$  is the velocity of electrons on the Fermi surface,  $\omega$  is the angular frequency of light.

We used the method of successive approximations. In the zeroth approximation, we assumed that  $\beta_1 = \beta_2 = 0$ . Next, we determined the value of  $N$  and selected such a value of  $v$  that  $N$  was independent of  $\lambda$ . This made it possible to find the quantities  $\beta_1$ ,  $\beta_2$ ,  $N$  and  $\nu_{\text{opt}}$  in the first approximation. The resultant values of  $N$  and  $\nu_{\text{opt}}$  were then used to find  $\beta_1$  and  $\beta_2$  in the second approxi-

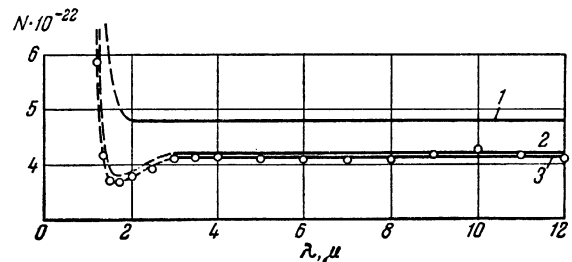


FIG. 5. Dependence of the value of  $N$  in Eq. (3) on  $\lambda$ . In the 3–12  $\mu$  region, this quantity represents the conduction electron density: 1)  $T = 293^\circ\text{K}$ ; 2)  $T = 78^\circ\text{K}$ ; 3)  $T = 4.2^\circ\text{K}$ . The experimental points refer to  $T = 293^\circ\text{K}$  and  $T = 78^\circ\text{K}$  because these values agree with those obtained earlier.<sup>[2]</sup>

Table II

$\lambda, \mu$	$T = 293^\circ \text{K}$				$T = 78^\circ \text{K}$				$T = 4.2^\circ \text{K}$			
	$\beta_1 \cdot 10^8$	$\beta_2 \cdot 10^8$	$N \cdot 10^{-22}$	$\nu_{\text{opt}} \cdot 10^{-14}$	$\beta_1 \cdot 10^8$	$\beta_2 \cdot 10^8$	$N \cdot 10^{-22}$	$\nu_{\text{opt}} \cdot 10^{-14}$	$\beta_1 \cdot 10^8$	$\beta_2 \cdot 10^8$	$N \cdot 10^{-22}$	$\nu_{\text{opt}} \cdot 10^{-14}$
2.5	0.40	3.34	4.69	3.81	0.18	7.82	3.97	1.63	0.12	8.0	3.91	1.33
3.0	0.48	3.97	4.73	3.19	0.19	10.7	4.16	1.19	0.13	10.7	4.12	0.99
3.5	0.58	4.37	4.70	2.84	0.20	12.8	4.20	1.05	0.16	11.9	4.17	0.88
4.0	0.68	4.77	4.66	2.59	0.22	14.8	4.22	0.83	0.16	14.4	4.19	0.71
5.0	0.93	5.17	4.75	2.36	0.34	14.6	4.14	0.83	0.19	17.2	4.13	0.58
6.0	1.2	5.26	4.76	2.26	0.44	15.8	4.16	0.76	0.26	18.0	4.11	0.54
7.0	1.6	5.11	4.79	2.24	0.58	16.4	4.22	0.73	0.33	18.6	4.12	0.53
8.0	1.9	4.91	4.79	2.24	0.72	16.8	4.24	0.71	0.40	19.5	4.13	0.50
9.0	2.2	4.75	4.78	2.23	0.91	16.6	4.15	0.71	0.55	18.8	4.20	0.52
0.0	2.5	4.48	4.77	2.26	1.2	15.4	4.06	0.76	0.73	17.8	4.23	0.55
1.0	2.9	4.24	4.83	2.30	1.6	13.8	4.11	0.84	0.96	16.6	4.21	0.60
2.0	3.2	3.98	5.00	2.36	2.0	12.3	4.10	0.87	1.2	15.1	4.11	0.64

Table III. Microproperties of tin\*

	$T = 293^\circ \text{K}$	$T = 78^\circ \text{K}$	$T = 4.2^\circ \text{K}$
$N$	$4.8 \cdot 10^{22}$	$4.2 \cdot 10^{22}$	$4.15 \cdot 10^{22}$
$N/N_a$	1.3 <sub>0</sub>	1.1 <sub>4</sub>	1.1 <sub>2</sub>
$\nu$	$0.93 \cdot 10^8$	$1.0 \cdot 10^8$	$0.85 \cdot 10^8$
$\nu_{\text{opt}}$	$2.26 \cdot 10^{14}$	$0.76 \cdot 10^{14}$	$0.56 \cdot 10^{14}$
$\nu_{\text{cl}}^{\text{ef}}$	$1.64 \cdot 10^{14}$	$0.28 \cdot 10^{14}$	—
$\nu^{\text{ed**}}$	$6 \cdot 10^{12}$	$5 \cdot 10^{12}$	$5 \cdot 10^{12}$
$\nu^{\text{ef}}$	$2.20 \cdot 10^{14}$	$0.70 \cdot 10^{14}$	$0.50 \cdot 10^{14}$
$l$	$0.4 \cdot 10^{-6}$	$1.3 \cdot 10^{-6}$	$1.5 \cdot 10^{-6}$
$\delta$	$2.8 \cdot 10^{-6}$	$2.7 \cdot 10^{-6}$	$2.6 \cdot 10^{-6}$

\*Here,  $N_a$  is the concentration of atoms;  $\nu^{\text{ed}}$  is the frequency of the collisions between electrons and impurities;  $\nu^{\text{ef}} = \nu_{\text{opt}} - \nu^{\text{ed}}$ ;  $l$  is the mean free path of electrons;  $\delta$  is the depth of the skin layer. All quantities are given in cgs esu.

\*\*The frequency of collisions between electron and impurities  $\nu^{\text{ed}}$  decreases on cooling due to the reduction of  $N$ .

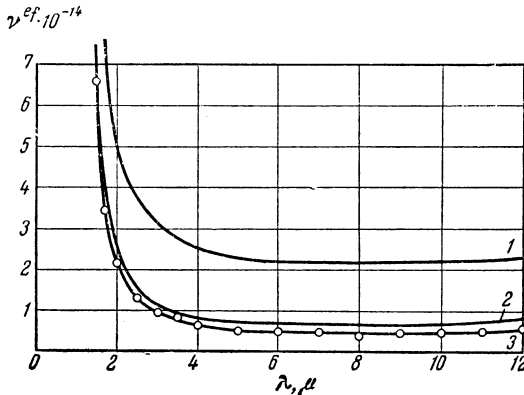


FIG. 6. Dependence of  $\nu^{\text{ef}}$  on  $\lambda$  at various temperatures: 1)  $T = 293^\circ \text{K}$ ; 2)  $T = 78^\circ \text{K}$ ; 3)  $T = 4.2^\circ \text{K}$ . The points refer to  $T = 4.2^\circ \text{K}$  (cf. the legend of Fig. 5).

mation, and these in turn were employed to determine  $N$ ,  $\nu_{\text{opt}}$  and  $\nu$  in the second approximation. The results of the third approximation were practically identical with those of the second. Table II lists the values of  $\beta_1$ ,  $\beta_2$ ,  $N$  and  $\nu_{\text{opt}}$  in the region  $\lambda = 2.5-12 \mu$ . The velocity  $\nu$ , which occurs in the expressions for  $\beta_1$  and  $\beta_2$ , was found by the least

squares method. This velocity is listed in Table III, which includes the average values of the other microproperties.

It was found that the conduction electron density in tin decreased on cooling (Fig. 5). This effect represented a variation of the overlap of the energy bands of tin with temperature. In other investigated metals (Al, Pb, Au, Ag, Cu<sup>[5,6]</sup>), the electron density did not vary with temperature. In tin, as shown by Table III and Fig. 5, the density changed considerably on cooling from room temperature to liquid-nitrogen temperature, and very little on cooling from nitrogen temperature to helium temperature.<sup>2)</sup>

The main purpose of our work was to check the temperature dependence of the electron-phonon collision frequency. Since the volume losses are proportional to  $\nu^{\text{ef}}$ , and the surface losses are proportional to  $\beta_2 \nu^{\text{ef}}$ , a determination of the dependence  $\nu^{\text{ef}}(T, \omega)$  will automatically give the dependence of the absorption on the same variables. Table III and Fig. 6 indicate that the dependence  $\nu^{\text{ef}}(T)$  confirms qualitatively the results which follow from the quantum transport equation. In fact,  $\nu^{\text{ef}}$  remains a large quantity, equal to  $0.5 \times 10^{14} \text{ sec}^{-1}$ , even at  $T = 4.2^\circ \text{K}$ . For quantitative comparison of the theoretical and experimental results, we shall use the ratio  $\nu^{\text{ef}}(T_1)/\nu^{\text{ef}}(T_2)$ . The experimental results allow us to use two temperature ranges: 293 to  $78^\circ \text{K}$ , and 78 to  $4.2^\circ \text{K}$ . For each of these ranges, we determined experimentally the parameter  $\Theta$  from the temperature de-

<sup>2)</sup>We are assuming that the reduction in the energy band overlap, which is observed in tin, is due to the temperature dependence of the lattice constant. Precisely this type of effect is expected from theoretical calculations of the dependence of the band overlap on the lattice constant of diamond-type crystals.<sup>[7]</sup>

pendence of the static conductivity of the investigated layers. For the former range  $\Theta = 187^\circ\text{K}$ , and for the latter  $\Theta = 128^\circ\text{K}$ .<sup>3)</sup> The corresponding values of  $\Theta$  obtained from the temperature dependence of the conductivity of bulk tin are, respectively,  $193\text{--}208^\circ\text{K}$  for the first temperature range, and  $131\text{--}137^\circ\text{K}$  for the second.<sup>[8]</sup> The determination of  $\Theta$  from measurements of the specific heat of the bulk metal gives approximately the same values.<sup>[9]</sup>

The dependence of the electron-phonon collision frequency on temperature according to theory and experiment has the form

Temperature range	$T_1\text{--}T_2, ^\circ\text{K}$ :	293—78	78—4.2
$v^{ef}(T_1)/v^{ef}(T_2)$ {	theory:	2.9	1.7
	experiment:	3.1	1.4

These results agree to within 20%. If we compare the experimental results with those obtained from the classical transport equation, we find that they differ by a factor of  $10^6$ .

The observed effect cannot be explained by the surface losses, which were allowed for using formulas (3)–(6). For tin, the surface losses even at helium temperature amount to only 20% of the volume losses. Therefore, some inaccuracy of these formulas, associated with the fact that they apply to a spherical Fermi surface, does not alter our results. The observed effect can likewise not be due to the losses associated with electron collisions with impurities and grain boundaries. These losses were found by us from the residual resistance: they amount only to 10% of the volume losses. Therefore, the slight error associated with this method of determination (the Matthiessen rule is assumed to be valid) again does not affect the results obtained.

<sup>3)</sup>In the determination of  $\Theta$  in the latter range of temperatures, we used the value of the conductivity at the temperature of liquid hydrogen  $\sigma_H = 1.6 \times 10^{18}$  cgs esu. This value is more accurate than that used in<sup>[2]</sup>.

Thus, our experimental data show that at helium temperatures the volume absorption in tin associated with the creation of the complete spectrum of phonons remains strong. The quantitative agreement between the experimental results and those found from the quantum transport equation may be regarded as satisfactory.

<sup>1</sup>R. N. Gurzhi, JETP **33**, 451, 660 (1957), Soviet Phys. JETP **6**, 352, 506 (1958); Dissertation, Physico-Technical Institute of the U.S.S.R. Academy of Sciences (1958).

<sup>2</sup>A. I. Golovashkin and G. P. Motulevich, JETP **46**, 460 (1964), Soviet Phys. JETP **19**, 310 (1964).

<sup>3</sup>Golovashkin, Motulevich, and Shubin, PTE No. 5, 74 (1960).

<sup>4</sup>M. Cardona and D. L. Greenaway, Phys. Rev. **125**, 1291 (1962).

<sup>5</sup>Golovashkin, Motulevich, and Shubin, JETP **38**, 51 (1960), Soviet Phys. JETP **11**, 38 (1960); A. I. Golovashkin and G. P. Motulevich, JETP **44**, 398 (1963), Soviet Phys. JETP **17**, 271 (1963).

<sup>6</sup>V. G. Padalka and I. N. Shklyarevskii, Optika i spektroskopiya **11**, 527 (1961); **12**, 291 (1962).

<sup>7</sup>J. Bardeen and W. Shockley, Phys. Rev. **80**, 72 (1950).

<sup>8</sup>Ya. G. Dorfman and S. É. Frish (ed.), Sbornik fizicheskikh konstant (Collection of Physical Constants), ONTI, 1937; Handbook of Chemistry and Physics, Cleveland, Ohio, 37th edition; C. J. Smithells, Metals Reference Book, 1955.

<sup>9</sup>Low Temperature Physics Handb. Physik v. XIV-XV, Springer, Berlin, 1956; J. Eisenstein, Revs. Modern Phys. **26**, 277 (1964).

Translated by A. Tybulewicz